

Temporal Spectrum Analysis for Multi-Constellation Space Domain Awareness

Mansour Naslcheraghi, Gunes Karabulut-Kurt

*Poly-Grames Research Center, Department of Electrical Engineering
Polytechnique Montréal, Montréal, Canada*

Abstract—Space Domain Awareness (SDA) system has different major aspects including continues and robust awareness from the network that is crucial for an efficient control over all actors in space. The observability of the space assets on the other hand requires efficient analysis on when and how observed space objects can be controlled. This becomes crucial when real-world spatial dynamics are taken into account as it introduces complexities into the system. The real-world dynamics can reveal the structure of the network including isolated and dominant stations. We propose a Temporal Spectrum Analysis (TSA) scheme that takes into account a set of real-world parameters including actual dynamics of the objects in space to analyze the structure of a ground-space network that inherits temporal spectrum as the key element of design. We study the potential interactions between multiple constellations using TSA and conduct a comprehensive real-world simulations to quantify the structure of the network. Numerical results show how the temporal spectrum of each satellite affects the intra- and inter-constellation network structure including interactions between ground stations and constellations.

Index Terms—Space Domain Awareness, Temporal Spectrum, Spatial Dynamics.

I. INTRODUCTION

As human activity in space has rapidly expanded, the space environment has become increasingly crowded and contested. With thousands of active satellites, countless pieces of debris, and new objects being launched regularly, consequently, potential for collisions and accidents has grown significantly. Incidents such as emergency collision avoidance execution by European Aeolus satellite with Starlink-44 [1] and rendezvous (only 58m) between Oneweb and Starlink [2] has been mitigated urgently by Oneweb, which altered the orbit of its satellite to avoid incidents such as the Iridium-Cosmos collision [3], which had created at least 1000 pieces of debris larger than 10 cm plus many smaller ones. On the other hand, the term “Space Domain Awareness” (SDA) emerged more recently as space became a contested domain involving not just physical objects but also geopolitical interests and potential threats [4]. SDA reflects a broader perspective and not just the tracking of space objects but also understanding the intentions and capabilities of different space actors including constellations in operation. These capabilities are crucial in sustainability of the space and it covers broad civil applications as well. SDA mechanisms often rely on complex automated control systems to control satellites, spacecraft, and other space assets. To design such network, it is important to understand the physical structure of real-world ground-space network, which can help in designing more robust and

resilient systems by facilitating precise planning before the incident, such as collision avoidance command executions or Telemetry, Tracking, and Control (TT & C) operations. There has been a few attempts recently [5]–[10] to address challenging problems in SDA. From exploiting vision-based sensors for real-time collision avoidance scenarios [5] to predict and determine the full state of the satellites on-orbit by classifying orbital states in large Low Earth Orbit (LEO) constellation [6], studying time series in space-ground network with respect to correlated frequencies between ground stations [7], decentralized decision making approach [8] to overcome connectivity and communication times to have an efficient sensor tasking to sense, communicate, and exchange signals when needed, to employing Machine Learning (ML) tools to plan a distributed and autonomous system [9] which can adapt itself to respond unfamiliar situations when needed. The key advantage if possible, is always to have an efficient state prediction, so a better task planning can be realized [10].

However, none of the existing works studied the actual time domain spectrum analysis, which is crucial to understand behavior of a multi-constellation system in real-time. We aim to study how the structure of an arbitrary network can be inferred from the potential interactions between satellites and ground stations. How system’s spatial dynamics imply certain conditions that shape the influence of one constellation on another. These questions form the basis of this paper, where we introduce Temporal Spectrum Analysis (TSA) as a technique to address them. The TSA can reveal the temporal structure of ground-space networks and can be applied to designing efficient and long-term mechanisms for various purposes such as resource allocation, routing, network optimization, and decision-making.

Contributions: We first introduce temporal spectrum, which is a pulse function evolving over time due to spatial dynamics of the object orbiting the earth as the central body, and it has a semi-deterministic pattern that follows a continues pulses of step function in certain intervals. This modeling captures the accurate visibility in ground-space network where a given ground station visits certain satellites on regular basis. To the best of our knowledge, such temporal spectrum modeling has no presence in current state of the art. Given an arbitrary set of satellites along with their dedicated ground stations, we are interested to formulate the structure (wiring) of the network to study the correlations in spectrum patterns. For instance, we can identify ground stations that share simultaneous temporal

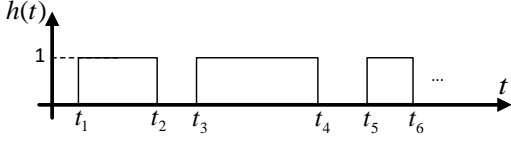


Fig. 1: Temporal spectrum $h(t)$ vs. time t .

spectrum to the same satellites or have complementary coverage patterns. We apply eigenvalue decomposition to derive information on ground stations with strongly overlapping satellite's temporal spectrum or isolated ones with less activity, which are major aspects of collective knowledge in a robust SDA system. We model possible interactions between multiple constellation which can be conveyed via temporal spectrum patterns between constellations. This interaction is modeled by pulse intensity which is a metric to quantify potential strength of a given constellation in observability of the target satellites, meaning that it will quantify behavior of the network in observing satellites throughout the time. The proposed framework is tested by a sophisticated inhouse framework designed for real-time SDA simulations. TSA technique is applied to a multi-constellation system composed of satellites from constellations Starlink, OneWeb, and Iridium and provide insights on the network structure for each individual constellation and multi-constellation system.

II. SYSTEM MODEL

Let us start defining the system of multiple constellations denoted by $C = \{c_1, c_2, \dots, c_{|C|}\}$, $|C|$ is the number of constellations and constellation c_i has its own dedicated ground stations denoted by set $G^{c_i} = \{g_1, g_2, \dots, g_{|G^{c_i}|}\}$, where $|G^{c_i}| \leq K$, $K \in \mathbb{N}$ is the number of ground stations in constellation c_i to handle a number of dedicated satellites denoted by the set $X^{c_i} = \{x_1, x_2, \dots, x_{|X^{c_i}|}\}$, $|X^{c_i}| \leq N$ for $N \in \mathbb{N}$.

A. Temporal Spectrum Modeling

Temporal spectrum is the actual physical time window from a ground station to a satellite on orbit and for an arbitrary pair of satellite $x_k \in X^{c_j}$ and ground station $g_i \in G^{c_j}$, it follows a continues pulse function denoted by $h_{ijk}(t)$ which has a shape of similar to the one illustrated in Fig. 1 (we omit indices in this figure for the sake of simplicity in demonstration). The pattern emerges from the spatial dynamics behavior of the system and the control/data signals can be exchanged within this temporal spectrum. For an arbitrary satellite denoted by x_k , t_m^{ijk} and t_{m+1}^{ijk} are start and end of one pulse which we can also call it "access window" and it has a length of Δt_m^{ijk} in seconds. There is no overlap between pulses in $h_{ijk}(t)$ because x_k never appears in two points of space, at a particular time, meaning that the pulse exists only when x_k is in line of sight with the ground station. Let us also explain why pulse duration is different as illustrated in Fig. 1. For instance, we can see that $t_2 - t_1 \neq t_4 - t_3 \neq t_6 - t_5$ for the same satellite w.r.t same

ground station. This is due to spatial dynamics of the system including earth rotation, satellite's orbits, and gravitational fields. We have taken all these real-world features into account in our real-time simulation platform with a reliability of up to sixty days and we will provide further details on this in the results section.

III. ANALYSIS

A real-world ground-space network is dynamic and duration of line of sight for each satellite associated to its ground station varies between different satellites. Thus, to start analyzing the ground-space network, we need to first determine a start and end time in which all objects in network have unanimous agreement on it, meaning that they are simultaneously operating within this time window. We call this window "simultaneity window" where every involving entity operate and form a network in operation. Having this time window in hand, we can determine the size of bitstream associated to each temporal spectrum which ultimately facilitates the follow-up operations. To do this, let us first write the continues-time temporal spectrum $h_{ijk}(t)$ as follows

$$h_{ijk}(t) = \sum_{m=1}^N \left[u(t - t_m) - u(t - t_m - \Delta t_m) \right], \quad (a), \quad (1)$$

where statement (a) : $t_{m+1} > t_m + \Delta t_m$ implies no overlap between pulses, t_m represents the starting time of the m -th pulse, Δt_m is the duration of the m -th pulse, N is the total number of pulses, and $t_{m+1} > \Delta t_m$ implies no overlap in temporal spectrum. And $u(t)$ is the unit step function defined as

$$u(t) = \begin{cases} 1, & t \geq 0, \\ 0, & t < 0. \end{cases}$$

Thus, the function $h_{ijk}(t)$ is a periodic sequence of pulses each with an amplitude of 1, separated by certain gaps. It is worth noting that the indices in time indicators are omitted for the sake of simplicity since they are different as we described earlier. Let us define unified global time T_g which spans from the earliest start time to the latest end time across all temporal spectrum for all ground stations and satellites as

$$T_g = [t_{\text{start}}^g, t_{\text{end}}^g], \quad (2)$$

where

$$t_{\text{start}}^g = \min\{t_{\text{start}}^i\}, \quad t_{\text{end}}^g = \max\{t_{\text{end}}^i\}, \quad (3)$$

where t_{start}^i and t_{end}^i are start/end of first/last pulses, respectively. Fig. 2 illustrates the graphical demonstration of the approach to determine the global time for three satellites visited by one ground station with varying pulse duration. Now, let us form discrete-time of the function in eq. (1) w.r.t global time window as

$$h_{ijk}[n] = \begin{cases} 1 & \text{if } n \in [t_m, t_m + \Delta t_m] \cap [t_{\text{start}}^i, t_{\text{end}}^i], \\ 0 & \text{otherwise.} \end{cases} \quad (4)$$

In fact, eq. (4) is a binary sequence where each bit represents one second of information in temporal spectrum, meaning that

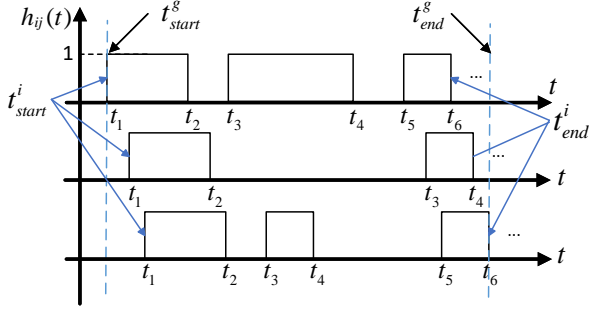


Fig. 2: Simultaneity conditions between observations.

for a given time instance $t = t_0$, the binary value is 1 if the satellite x_k is in line of sight with ground station g_i in constellation j , and 0 otherwise. It is worth noting that one can tune the precision of sampling by $\alpha \geq 1$ seconds by $h_{ijk}[m] = h_{ijk}[\alpha \cdot m]$ subject to meeting nyquist conditions, yet here we assume none-sampled signal for the sake of simplicity. Now, let us define a matrix \mathbf{H}^{c_j} as the temporal spectrum strength between all ground stations in constellation c_j and satellites X^{c_j} as

$$\mathbf{H}^{c_j} = \begin{bmatrix} \hat{h}_{1c_j1} & \hat{h}_{1c_j2} & \dots & \hat{h}_{1c_j|X^{c_j}|} \\ \hat{h}_{2c_j1} & \hat{h}_{2c_j2} & \dots & \hat{h}_{2c_j|X^{c_j}|} \\ \vdots & \vdots & \ddots & \vdots \\ \hat{h}_{|G^{c_j}|c_j1} & \hat{h}_{|G^{c_j}|c_j2} & \dots & \hat{h}_{|G^{c_j}|c_j|X^{c_j}|} \end{bmatrix}, \quad (5)$$

with size of $|G^{c_j}| \times |X^{c_j}|$ and each element \hat{h}_{ic_jk} is total time associated to temporal spectrum between ground station g_i and satellite x_j and it is specified by

$$\hat{h}_{ic_jk} = \sum_{n=t_{\text{start}}^g}^{t_{\text{end}}^g} h_{ic_jk}[n] \quad \text{seconds}, \quad (6)$$

where $h_{ic_jk}[n]$ is given by eq. (4) and $\hat{h}_{ic_jk} \leq T_g$ since the overall observable window cannot exceed the global time.

A. Intra-Constellation Dominant and Isolated Stations

Eigenvalue decomposition of the matrix \mathbf{H}^{c_j} reveals critical structural properties of the network. Large eigenvalues indicate redundant temporal spectrum patterns, while small eigenvalues highlight inefficiencies or limited *access windows*. To analyze this, we examine $\mathbf{J} = \mathbf{H}^{c_j} \mathbf{H}^{c_jT}$, where \mathbf{H}^{c_jT} is the transpose of \mathbf{H}^{c_j} . This provides insights into satellite-ground station relationships and the overall robustness of the SDA network. In fact, the matrix \mathbf{J} quantifies the total *access window* overlap or energy (strength) across ground stations in constellation c_j . Diagonal entries \mathcal{J}_{ii} represent the observation strength of individual stations, in which higher values indicate redundancy. Off-diagonal entries \mathcal{J}_{ij} ($i \neq j$) measure temporal spectrum overlap between stations g_i and g_j , in which large values illustrates redundant coverage patterns. Now, by decomposing \mathbf{J} through

$$\mathbf{J} = \mathbf{Q} \mathbf{\Lambda} \mathbf{Q}^T, \quad (7)$$

where we obtain $\mathbf{\Lambda}$, which is a diagonal matrix of eigenvalues, which corresponds to variance in observation modes, and \mathbf{Q} is an orthogonal eigenvector matrix, which captures interaction or redundancy among stations. The dominant and isolated ground stations g_i is identified by

$$\hat{i} = \arg \max_{i \in \{1, 2, \dots, |G^{c_j}|\}} \lambda_i, \quad \tilde{i} = \arg \min_{i \in \{1, 2, \dots, |G^{c_j}|\}} \lambda_i. \quad (8)$$

These stations, $g_{\hat{i}}$ and $g_{\tilde{i}}$, are pivotal for load balancing in constellation c_j . The complete procedure is outlined in algorithm 1.

Algorithm 1: Dominant and Isolated Stations (Intra)

Require: G^{c_j} , X^{c_j} , t_m , Δt_m , t_{start}^i , t_{end}^i
Ensure: dominant $g_{\hat{i}}$ and isolated $g_{\tilde{i}}$

- 1: Solve (3) and get global time window T_g
- 2: Initialize matrix \mathbf{H}^{c_j}
- 3: **for** each station $g_i \in G^{c_j}$ **do**
- 4: **for** each satellite in $x_j \in X^{c_j}$ **do**
- 5: Get $h_{ic_jk}[n]$ using eq. (4)
- 6: Calculate \hat{h}_{ic_jk} using eq. (6) and form \mathbf{H}^{c_j}
- 7: **end for**
- 8: **end for**
- 9: Calculate $\mathbf{J} = \mathbf{H}^{c_j} \mathbf{H}^{c_jT}$
- 10: Solve $\det(\mathbf{J} - \lambda \mathbf{I}) = 0$ as in (7) and get λ_i
- 11: Solve eqs. (8)
- 12: **return** $g_{\hat{i}}$ and $g_{\tilde{i}}$

B. Inter-Constellation Temporal Interaction

To quantify the role of each constellation in temporal spectrum pattern, we introduce a metric that captures the interaction dynamics between constellations. Specifically, we define *pulse intensity* as the frequency at which a typical satellite is accessed by a ground station. This metric embeds inter-constellation information flow and emergency response capabilities. The *pulse density* ρ_{ij} measures how frequently satellites in constellation X^{c_j} are accessed by ground stations in constellation G^{c_i} . It is defined as the number of pulses per unit time, irrespective of pulse duration:

$$\rho_{ij} = \frac{\mathcal{P}_{ij}}{T_g} \quad \text{pulses/second}, \quad (9)$$

where \mathcal{P}_{ij} is total number of pulses given by

$$\mathcal{P}_{ij} = \sum_{n=t_{\text{start}}^i+1}^{t_{\text{end}}^i} [h_{ic_jj}[n] - h_{ic_jj}[n-1]]^+, \quad (10)$$

where $[x]^+ = \max(0, x)$ counts only positive transitions from 0 to 1. The distribution of pulses across constellations, namely distribution of ρ_{ij} follows a probability mass function (PMF) denoted by $f_{i \rightarrow j}(k)$ that relies on spatial dynamics of the system, where $k = \lceil \frac{\rho_{ij}}{60} \rceil$ is the number of pulses per hour for the interaction from constellation c_i to c_j . $\lceil x \rceil$ gives the smallest integer greater than or equal to x . This

PMF is derived empirically from real-time simulations, which captures the likelihood of observing ρ_{ij} pulses in a given time frame. However, to quantify the structure of the network in terms of the pulses, we can identify the ground station g_i with the highest number of pulses for a given satellite and time interval. With this choice, we make the strongest choice for interaction from one constellation into another which illustrates the strongest representation from a constellation and it is defined by

$$P_{ij} = \max_{i \in \{1, \dots, |G^{c_i}|\}} \sum_{l=1}^{|X^{c_j}|} \mathcal{P}_{ij}. \quad (11)$$

Next, let us utilize P_{ij} and construct the *interaction intensity* matrix \mathbf{P} as follows.

$$\mathbf{P} = \begin{bmatrix} P_{11} & P_{12} & \dots & P_{1|C|} \\ P_{21} & P_{22} & \dots & P_{2|C|} \\ \vdots & \vdots & \ddots & \vdots \\ P_{|C|1} & P_{|C|2} & \dots & P_{|C||C|} \end{bmatrix}_{|C| \times |C|}, \quad (12)$$

where $|C|$ is the number of constellations. To analyze the interactions between constellations, again we perform eigenvalue decomposition on \mathbf{P} as

$$\mathbf{P}\vec{v}_i = \gamma_i \vec{v}_i, \quad i = 1, 2, \dots, |C|, \quad (13)$$

where γ_i are the eigenvalues and \vec{v}_i are the corresponding eigenvectors. A large γ_{\max} indicates strong overall connectivity between constellations, while \vec{v}_{\max} associated with γ_{\max} reveals the relative contribution of each constellation to the dominant interaction mode.

IV. NUMERICAL RESULTS

Numerical results are conducted in an inhouse real-time platform that integrates Simplified General Perturbations 4 (SGP4) [11] and High Precision Orbital Propagator (HPOP) from STK platform [12]. These are widely used orbit propagators where SGP4 gives prediction reliability up to four days and HPOP gives reliable propagation for up to sixty days. Satellites are sampled from real-world data source CellesTrak [13] for constellations Oneweb, Starlink, and Iridium. Full spatial dynamics are taken into account from Two-line element (TLE) set [13]. First, let us illustrate the temporal spectrum in action which is delineated in Fig. 3. This is for satellite Oneweb-12 vs. International Ground Station (IGS) Alice Springs, meaning that if Oneweb-12 was allowed to communicate with this IGS station, demonstration shows the moments that visibility was possible. In practice, Oneweb is not using IGS and this is just a sample scenario in our study, which is similar for every other pairs of satellites and ground stations. First, *Scenario A*, to evaluate algorithm 1. We obtained dominant ground stations (\bar{g}_i) and we omit demonstration of weak ground stations (\bar{g}_i) due to lack of space. We have deployed network composed of IGS network (39 Stations), constellations Oneweb (651 Satellites), Starlink (6909 Satellites), and Iridium (30 Satellites), with the precision of $\alpha = 1$ second and duration of 2 hours. Fig. 4 delineates the

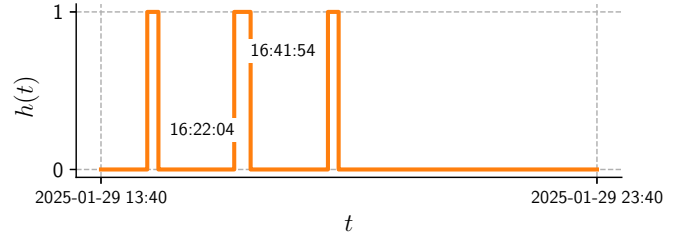


Fig. 3: Temporal spectrum $h(t)$ for Oneweb-12 vs. ground station Alice Springs, Australia (ASA/ASN).

TABLE I: simulation parameters for scenario B

Parameters	Values: Oneweb, Starlink, Iridium
Number of Satellites	30, 50, 20
Ground Stations	10, 20, 4
Altitude (Km)	$\sim 1200, 600, 780$
Orbital Propagator	SGP4 and HPOP for all
Period (minutes)	$\sim 109, 90, 100$
Inclination (degree)	$\sim 89^\circ, 53^\circ, 86^\circ$
Mean Motion (rev/day)	$\sim 13.15, 15, 14.5$
Simulation Duration (hours)	10

results where algorithm 1 is executed for each constellation separately. It takes memory of size $\frac{|G^{c_j}| |X^{c_j}| (t_{\text{end}}^g - t_{\text{start}}^g) \times 3600}{\alpha}$ bits to build matrix \mathbf{H}^{c_j} . We demonstrated top three stations which have the highest visibility to all constellations yet with some differences in strength due to nature of spatial dynamics between constellations. Next, *Scenario B*, to evaluate pulse distributions, namely PMFs $f_{i \rightarrow j}(k)$. Network of ground stations in multiple countries across the globe are deployed to have global coverage. Table I summarizes some of the key parameters for this scenario. Fig. 5 demonstrates the PMF of pulses for stations of different constellations against its own satellites and satellites from other constellations. We observe that for a given constellation, there is temporal spectrum available to another constellation with variable number of pulses. We can also observe similarities for all of constellations around 2-4 pulses on average with highest probability. The reason is that for LEO orbit within 10 hours, satellites can make at least two complete orbits around the earth. Let us focus on one particular behavior here. Oneweb and Starlink stations potentially have highest interactions with Iridium satellites as illustrated in Fig. 5 (a), (b) due to frequent line of sights from these constellations to Iridium satellites.

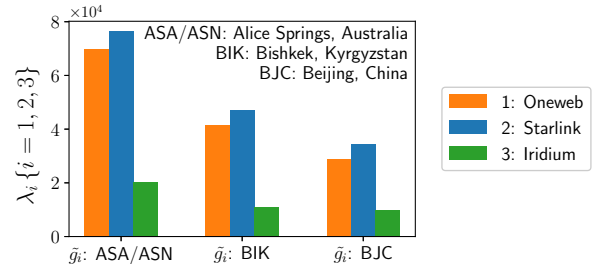


Fig. 4: Top three dominant stations for all constellations.

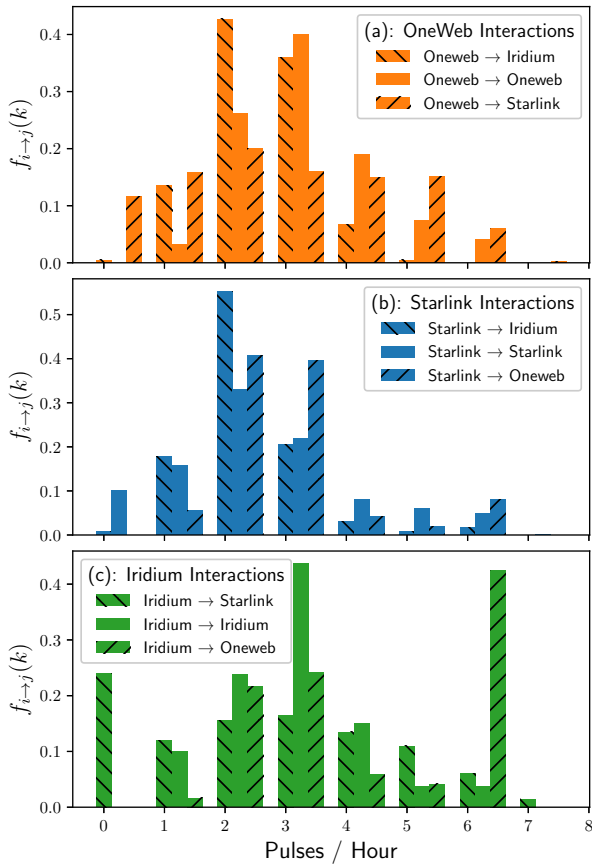


Fig. 5: PMF of pulses per hour for different constellations.

Similarly, Iridium has highest probability of visiting satellites from Oneweb as illustrated in (c). These behaviors shows how we can infer about the physical structure of a space-ground network and plan complicated tasks ahead of time.

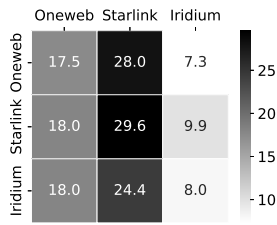


Fig. 6: Interaction intensity matrix \mathbf{P} .

Finally, Fig. 6 demonstrates the interaction intensity between constellations which is encoded by *interaction intensity* when most frequent pulses are taken into account. This is the matrix \mathbf{P} as in eq. (12) and we can see that Starlink have the highest pulse intensity, meaning that Starlink's ground stations visits its satellites more frequently. As for the inter-constellation interactions, Iridium has the lowest interaction values since it is relatively small constellation with limited temporal spectrum available to other constellations. Obtaining eigenvalues and eigenvectors of the adjacency matrix \mathbf{P} reveal key insights into

the visibility network of the three constellations. The dominant eigenvalue ($\gamma_1 = 55.1$) indicates strong overall connectivity with the eigenvector showing that all three constellations contribute significantly, especially Starlink (0.62), which is the most influential one. The complex conjugate eigenvalues ($\gamma_2 = -0.02 + 1.96j$, $\gamma_3 = 0.02 - 1.95j$) is cyclic visibility pattern with the Iridium (0.74) playing a central role in these patterns, which they persist over time due to small real parts. Overall, the network exhibits robust connectivity with periodic visibility dynamics. One can also see Fig. 6 as the weights of a directed graph where each weight presents the interaction intensity from one constellation into another, in which it has a physical reality in real-world if constellations would share this temporal spectrum with each other over their ground stations.

V. CONCLUDING REMARKS

Space Domain Awareness is crucial for sustainability and due to increasing threats to space assets, space actors share responsibilities and in this paper, we have analyzed potential interactions not only within individual constellation but also between constellations. By analyzing the temporal spectrum, we demonstrated how we can derive information on actual structure of the network along with potential interactions. These interactions are crucial to design a robust SDA system that requires efficient handling of control signals. The temporal spectrum analysis reveals temporal structure of ground-space network and can be applied to designing efficient and long-term mechanisms for various purposes such as resource allocation, routing, network optimizations, and decision makings.

REFERENCES

- [1] ESA Space Safety, *Predicted near miss between Aeolus and Starlink 44*, https://www.esa.int/ESA_Multimedia/Images/2019/09/Predicted_near_miss_between_Aeolus_and_Starlink_44.
- [2] Science X network, *Starlink and OneWeb have their first avoidance maneuver with each other's constellations*, <https://phys.org/news/2021-05-starlink-oneweb-maneuver-constellations.html>.
- [3] Wikipedia, *2009 satellite collision*, https://en.wikipedia.org/wiki/2009_satellite_collision.
- [4] Mariel Borowitz, *From Space Situational Awareness to Space Domain Awareness*, in *The Militarization of European Space Policy*, Taylor & Francis, 2023.
- [5] Khaja Faisal Hussain, Kathiravan Thangavel, Alessandro Gardi, and Roberto Sabatini, *Real-Time Resident Space Object Surveillance Using Distributed Satellite Systems*, in *2023 IEEE/AIAA 42nd Digital Avionics Systems Conference (DASC)*, pp. 1–9, IEEE, 2023.
- [6] Dongfang Wang and Fen Li, *A machine learning method for the orbit state classification of large LEO constellation satellites*, *Advances in Space Research*, vol. 71, no. 3, pp. 1644–1656, 2023.
- [7] Yujiao Niu, Paul Rebischung, Min Li, Na Wei, Chuang Shi, and Zuheir Altamimi, *Temporal spectrum of spatial correlations between GNSS station position time series*, *Journal of Geodesy*, vol. 97, no. 2, p. 12, 2023.
- [8] Samuel Fedeler, Marcus Holzinger, and William Whitacre, *Decentralized decision making over random graphs for space domain awareness*, *Advances in Space Research*, vol. 73, no. 10, pp. 5266–5283, 2024.
- [9] Samuel Hilton, Kathiravan Thangavel, Alessandro Gardi, and Roberto Sabatini, *Intelligent mission planning for autonomous distributed satellite systems*, *Acta Astronautica*, vol. 225, pp. 857–869, 2024.
- [10] Nathaniel G. Gordon, Nesrine Benchoubane, Gunes Karabulut-Kurt, and Gregory Falco, *On the Role of Communications for Space Domain Awareness*, *arXiv preprint arXiv:2406.05582*, 2024.
- [11] David Vallado and Paul Crawford, *SGP4 orbit determination*, in *AIAA/AAS Astrodynamics Specialist Conference and Exhibit*, p. 6770, 2008.

- [12] Ansys, *High Precision Orbital Propagator (HPOP)*, <https://help.agi.com/stk/#hpop/hpop.htm>.
- [13] T.S. Kelso, *NORAD GP Element Sets Current Data*, <http://celestrak.org/NORAD/elements/>.